Occurrence of salt water above fresh water in dynamic equilibrium in a coastal groundwater flow system near De Panne, Belgium

A. Vandenbohede · L. Lebbe

Abstract A salt water lens is found above fresh water under the shore between Dunkerque (France) and Nieuwpoort (Belgium). This inverse density distribution is in a dynamic equilibrium. It develops due to the infiltration of salt water on the back shore during high tide. Under this salt water lens, water infiltrated in the adjacent dune area flows towards the sea and discharges at the seabed. This water quality distribution differs from the classic salt water wedge under fresh water described in the literature. Here, the evolution to this water quality distribution is simulated with a density dependent numerical model. A large tidal range, shore morphology and a permeable groundwater reservoir are the main conditions for the observed water quality distribution. By altering these conditions, intermediate water quality distributions between the classic salt water wedge and the one discussed here develop. Based on these simulations, it is expected that similar kinds of inverse density distribution could be present in a number of coastal areas, which have tides, a gently sloping shore and a permeable substratum.

Résumé On a trouvé dans un aquifère côtier, situé entre Dunkerque (France) et Nieuwpoort (Belgique) une lentille d'eau salée au dessus de l'eau douce. Cette distribution inverse de la densité se trouve dans un équilibre dynamique. Elle se développe à cause des infiltrations d'eau salée pendant la haute marée. Au dessous de ces lentilles d'eau salée, l'eau infiltrée au long de dunes se dirige vers la mer et se décharge au fonds de la mer. Cette distribution de la qualité des eaux diffère de biseau d'eau salée classique présentée dans la littérature. Dans cet article l'évaluation de la distribution de la qualité de l'eau est simulée avec un modèle numérique à densité variable. Les conditions principales considérées pour analyser la distribution observée de la qualité de l'eau ont été un grand intervalle de variation pour la marée, la morphologie de la côte et un réservoir perméable d'eau souterraine. En alternant cettes conditions on a mis en évidence dans la distribution de la qualité de l'eau des stages intermédiaires entre le biseau classique et la situation présentée auparavant. À partir des simulations on peut considérer qu'il est possible d'avoir des distributions inverses de la densité dans des aquifères côtières dans la présence des marées et dans des conditions d'une côte à pente douce et d'une couche perméable.

Resumen Se encontró un lente de agua salada sobre agua dulce, debajo de la zona litoral entre Dunkerke (Francia) y Nieuwpoort (Bélgica). Esta distribución invertida de la densidad está en equilibrio dinámico. Se desarrolla debido a la infiltración del agua salada sobre la zona emergida de la playa (berma de playa), durante los episodios de marea alta. Bajo este lente de agua salada, el agua infiltrada en el área de dunas adyacente, fluye hacia el mar y descarga en el lecho marino. Esta distribución de calidad de agua, es diferente de la clásica cuña de agua salada bajo el agua dulce descrita en la literatura. La evolución para esta distribución de calidad de agua se simuló con un modelo numérico de densidad dependiente. Las principales condiciones para la distribución observada de calidad de agua son: Un rango amplio de mareas, la morfología de la zona costera y un reservorio permeable de agua subterránea. Cuando se alteran estas condiciones, se desarrollan distribuciones intermedias de calidad de agua, oscilando entre la cuña de agua salada clásica y el modelo aquí discutido. Con base en estas simulaciones se espera que tipos similares de distribución de densidad invertida, podrían estar presentes en un número de áreas costeras, que tengan mareas, una pendiente litoral suave y un sustrato permeable.

Keywords Coastal aquifers · Salt-water/fresh-water relations · Numerical modelling

Received: 10 June 2004 / Accepted: 20 January 2005
Published online: 9 April 2005

A. Vandenbohede (✉) · L. Lebbe
Department Geology and Soil Science, Ghent University,
Krijgslaan 281 (S8),
B-9000 Gent, Belgium
e-mail: alexander.vandenbohede@ugent.be
Tel.: +32-(0)9-2644652
Fax: +32-(0)9-2644652

Introduction

In coastal areas fresh groundwater flowing from land towards the sea comes in contact with salt sea water. A transition zone between the fresh and salt groundwater develops

 DOI 10.1007/s10040-005-0446-5

because of mixing. The position of this transition zone is dependent on local circumstances. A situation often found in textbooks (Bear 1972; Domenico and Schwartz 1998; Freeze and Cherry 1979; Rushton 2003) is the one where the transition zone is inclined landwards. Fresh water infiltrates on land, flows towards the sea and discharges on the land-sea border. Because of the density differences, a fresh water lens is found above a salt sea water wedge. This is a situation observed in many sites all over the world (Cooper et al. 1964; Pranzini 2002; Stuyfzand 1993). The hydraulic heads on land relative to the sea level together with aquifer characteristics determine the position of the transition zone. The sea level is hereby considered fixed at a mean value. However, the shore's topography, occurrence of tides and the hydraulic conductivity of the aquifer can make the distribution of fresh and salt water totally different. In the western Belgian coastal plain, salt water is found above fresh water under the shore. This inverse and, at first thought unstable density distribution is, however, in a dynamic equilibrium. This paper aims to describe this particular water quality distribution in its hydrogeological context. Combination of simulations with a mathematical model and water quality analyses shows the origin and evolution of the water quality distribution. A second set of simulations illustrates the effects of shore topography and tides on the water quality distribution. Finally, the influence of a semi-permeable layer in the groundwater reservoir is considered.

Geological setting of the shore and dunes in the western Belgian coastal plain

The study area is situated in the dune and shore area of the western Belgian coastal plain, along the French-Belgian border (Fig. 1). Geographically, it is part of the north-west European coastal dunes, which form a long, narrow dune strip from Calais (France) to the north of Denmark. The Belgian dunes can be divided into young dunes, formed between the 8th century and present and older dunes formed between 2000 and 5000 years ago. The young dunes have lime-rich, basic or neutral soils resulting in a unique flora. The shore is a tidal dominated sandy runnel and ridge type with a mean slope of about 1.1%. Runnels are depressions between the ridges and this type of beach profile is typical for shallow gradient beaches. It is covered by semi-diurnal tides. The difference between the high and low tide is at spring tide approximately 5 m and at neap tide 3 m. The sea level reaches its highest point at +5 mTAW and its lowest point at 0 mTAW (the Belgian ordnance datum level mTAW refers to mean low low sea water level, about 2.3 m below mean sea level). The horizontal distance between the mean high-tide line and the mean low-tide line ranges between 300 to 450 m. The distance between the dunes and the mean high-tide line is between 50 to 100 m. This part of the shore is only inundated during high sea levels. On the landward side, a low lying polder area borders the dune belt.

The current dune belt, the young dunes, started to form from the 7th or 8th century on. This formation took place in several phases. The first phase was a mobile dune phase

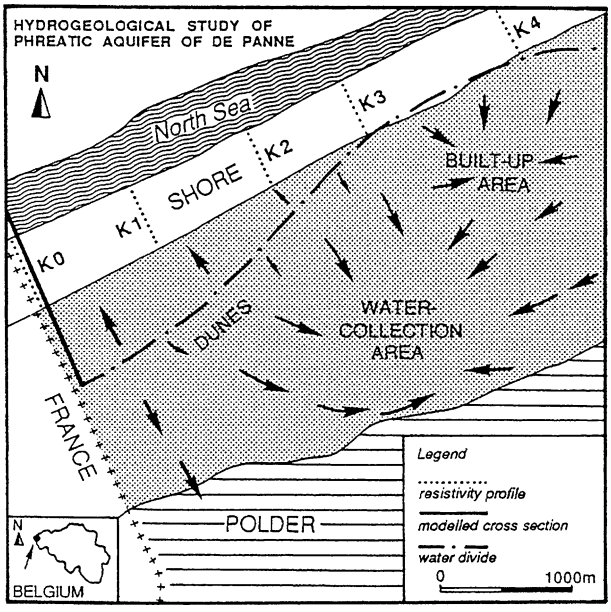

Fig. 1 Localisation of the studied area and of the KO resistivity profile along the French-Belgian border. General groundwater flow in the dunes towards the sea, polder and water collection area of De Panne is indicated

during the 9th to 10th century followed by a parabolic dune phase. The lower substratum of the thirty meter thick phreatic aquifer is formed by clay of the Kortrijk Formation, Ieper Group. These sediments are of early Eocene age and are considered impermeable in this study. The lower part of the phreatic aquifer consists of medium to coarse medium sands of Eemian age. Fine medium sands form the larger part of the aquifer. Lenses of silty fine sand can occur locally. The top of the aquifer consists of medium sands.

Previous work

Studies on water quality and groundwater flow in the western coastal plain have a longstanding tradition. Lebbe (1978) executed the first detailed hydrogeological study of the dune area. One of the findings was the occurrence of salt water above fresh water on the shore in the area of the high-water mark. Lebbe (1981) further studied this water quality distribution. Therefore, 30 rotary drillings were made along five cross-sections perpendicular to the shoreline. Resistivity logs (long normal method) were performed in each of these boreholes. Water quality analyses and time series of the hydraulic heads were made in a selection of these boreholes (Lebbe 1981).

Figure 2 shows the resistivity profile K0, situated along the French-Belgian border. Three resistivity classes are indicated representing fresh, brackish and salt water. The dunes are filled with fresh groundwater. Salt water is present directly under the shore. This becomes brackish deeper in the groundwater reservoir. In the deepest part fresh water is observed. This is the case for all four resistivity logs on the shore. From these logs, it is deduced that a salt water lens is present above a fresh water tongue emanating from

 DOI 10.1007/s10040-005-0446-5

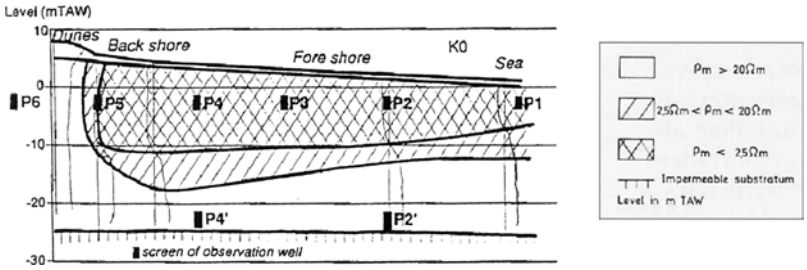

Fig. 2 Resistivity (ρ_m) profile KO along the French-Belgian border. The length of the profile is 430 m. Three resistivity classes are indicated corresponding with fresh ($\rho_m > 20$ Ωm), brackish (2.5 Ωm $< \rho_m < 20$ Ωm) and salt water ($\rho_m < 2.5$ Ωm)

the dunes and stretching out towards the sea. Modelling (Lebbe 1981; Lebbe 1983; Lebbe 1999) showed that this inverse distribution is in a dynamical equilibrium. This will be more thoroughly explained with the model described in this paper. The current work builds further on this previous work and aims to integrate the different observations of hydraulic heads, water quality analyses and geophysical borehole measurements in a new mathematical model to better understand the occurrence of fresh and salt water and its transition zone in coastal areas. Moreover, the influence of tidal range, shore width and a semi-permeable layer are simulated.

Water quality observations

Water analyses are available from observation wells P6, P5, P4, P4′, P2 and P2′. Concentrations of major cations and anions and water types are summarised in Table 1. Water types are determined following the Stuyfzand method (Stuyfzand 1986) classifying waters in main types, types, subtypes and classes using a code. The main type is determined by the chloride concentration. Fresh (F, 30–150 mg/l Cl^-), brackish (B, 300–1000 mg/l Cl^-), salt (S, 10000–20000 mg/l Cl^-), hyperhaline (H, >20000 mg/l Cl^-) and intermediate stages (F_b, B_s) are considered. Total hardness determines the type. Very soft (code 0) to extremely hard water (code 9) are considered. The most important cations and anions determine the subtype. The sum of Na^+, K^+ and Mg^{2+} in meq/l corrected for a contribution of seawater (this is the base exchange index) determines the class. With freshening the class becomes positive due to cation exchange. With salinization, the reverse is true. Fresh $CaHCO_3Ø$ water is found in the dunes and in the proximal part of the fresh water tongue. In P2′ mixing between fresh dune water and salt sea water is observed resulting in slightly brackish NaClØ water. Salt NaClØ is present in the salt water lens. P5 indicates the mixing of fresh dune water and salt sea water on the upper part of the back shore. Notice that all base exchange indexes are zero meaning that no cation exchange is actually taking place.

MOCDENS3D model

Boundary conditions and parameter values

MOCDENS3D (Oude Essink 2001) is used to model groundwater flow and solute transport. This model is applied because of its ability to accurately model density dependent groundwater flow and solute transport. MOCDENS3D is based on the three-dimensional solute transport code MOC3D (Konikow et al. 1996), but adapted for density differences. Three-dimensional flow in MOCDENS3D is described by the following equation:

$$\frac{\partial qx}{\partial x} + \frac{\partial qy}{\partial y} + \frac{\partial qz}{\partial z} - W = Ss * \frac{\partial hf}{\partial t}$$

x, y and z are coordinate directions; q_x, q_y and q_z are Darcian flow velocities (m/d) in x, y and z direction; W (d^{-1}) is a flux term accounting for pumping, recharge, or other sources and sinks; h_f is the fresh water head (m); S_s is the specific elastic storage (m^{-1}) and t is time (d). The Darcy velocity components are given by:

$$qx = -Kfx * \frac{\mu f * \partial hf}{\mu i * \partial x}$$

$$qy = -Kfy * \frac{\mu f * \partial hf}{\mu i * \partial y}$$

$$qz = -Kfz * \left(\frac{\partial hf}{\partial z} + \frac{\rho i - \rho f}{\rho f} \right)$$

Table 1 Concentration of major cations and anions (mg/l) and water type of water samples P6, P5, P4, P4′, P2 and P2′

	Na^+	K^+	Ca^{2+}	Mg^{2+}	Cl^-	SO_4^{2-}	HCO_3^-	Water type
P6	18.2	2.1	4.3	97.5	32.4	40.8	258	F2CaHCO$_3$Ã
P5	1917	61.7	213	229	3646	588	215	B$_s$NaClÃ
P4	7304	338	251	1120	13620	2194	162	S6NaClÃ
P4′	70.0	3.8	83.3	7.9	91.4	31.5	290	F2CaHCO$_3$Ã
P2	8272	366	317	1175	15670	2452	201	S6NaClÃ
P2′	256	17.0	127	36.2	512	134	250	B3NaClÃ

 DOI 10.1007/s10040-005-0446-5

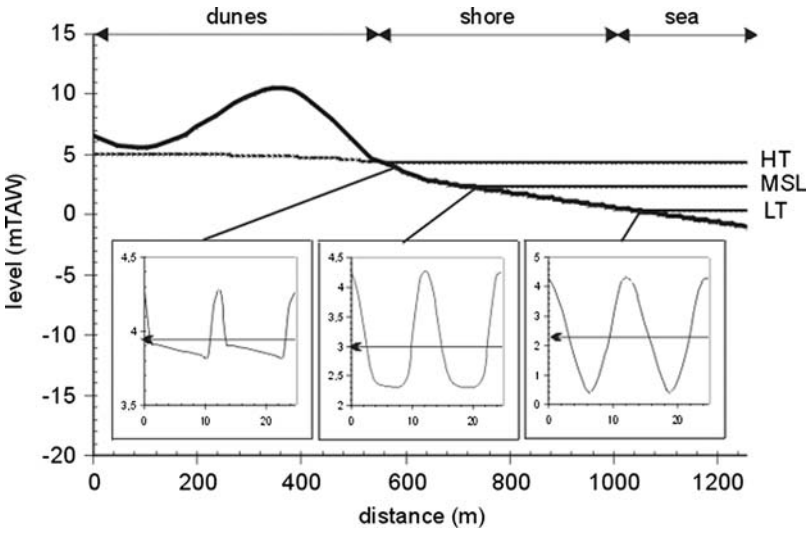

Fig. 3 Diagram of the modelled cross-section with indication of the dunes; shore; sea; sea level during high tide (HT), low tide (LT) and mean sea level (MSL); topography of the dunes, shore and sea bed and the water table in the dunes (dotted line) during high tide. The evolution of the fresh water head (mTAW) in function of time (h) for shallow observation wells placed just below the high tide mark, on mean sea level and on the low tide mark are given. The time averaged mean is indicated with an arrow. These are calculated heads based on the tides and the topography

μ_f and μ_i are the dynamic viscosity (kg/md) of fresh water and water at the *i*th point respectively; ρ_f and ρ_i are the densities (kg/m^3) respectively of fresh water and water at the same point; K_{fx}, K_{fy} and K_{fz} are fresh water horizontal hydraulic conductivities (m/d) and g is the acceleration due to gravity (m/d^2). Fresh water heads are used to cope with the different densities of waters. Groundwater flow can be simulated in an aquifer where density differences of groundwater occur and variations in hydraulic parameters within one layer and/or between different layers can be included. The groundwater flow equation is solved by the MODFLOW code taking into account density differences using a buoyancy term $((\rho_i - \rho_f)/\rho_f)$ in the basic flow equations. This buoyancy is related to concentrations through the equation of state:

$$\rho = \rho f\left(1 + \frac{\rho s - \rho f}{\rho f} * \frac{Ci, j, k}{Cs}\right)$$

where $C_{i,j,k}$ is the concentration (mg/l) of the *i*th row, *j*th column and *k*th layer in the model, C_s is the concentration (mg/l) of salt water and ρ_s is the density of salt water (kg/m^3). The advection-dispersion equation is solved by the methods of characteristics (Konikow and Bredehoeft 1978).

A 2D steady state groundwater flow and solute transport model was made with MOCDENS3D of the cross-section along the French-Belgian border. The aim of the modelling here is to visualise the evolution of the water quality distribution and the factors influencing it. The model consists of 30 layers and 126 columns, so the grid has 3780 cells. Every cell has a width of 10 m and a thickness of 1.0 m. The model grid has a width of 1260 m and is 30 m thick. It is divided into three parts, namely the dunes, shore and the sea (Fig. 3). The dunes, shore and sea have a width of respectively 540 m (columns 1 to 54), 420 m (columns 55 to 96) and 300 m (columns 97–126). The shore is defined here as the zone between maximum high tide and minimum low tide mark.

The aquifer is bounded below by clay of the Kortrijk Formation, which is here considered as an impermeable boundary. The landward vertical boundary is a no-flow boundary, coinciding with the water divide in the dunes. The upper boundary is partially located in the dunes, the shore and the sea. In the dunes a constant vertical flow boundary is used with an infiltration rate of 280 mm fresh water (TDS of 500 mg/l) per year (Lebbe 1978). A constant fresh water head boundary is set on the shore and the sea. For the sea, this is the mean sea level of 2.36 mTAW recalculated to fresh water heads and taking into account the gentle dipping of the seabed. Special care must be taken to determine the values for these constant heads on the shore due to the tides. The general distribution of fresh and salt groundwater is not determined by the daily tidal fluctuations but by the long term presence of tides on a gently sloping shore (Vandenbohede 2003) due to the small average interstitial velocities of the groundwater. It is therefore not needed to include the tides directly in the model but instead the mean time averaged fresh water heads on the top of the shore. This is illustrated in Fig. 3 where the evolution of the fresh water heads are given in function of time for a shallow observation well placed just below the high tide mark, on the low tide mark and around mean sea level. The observation well placed on the low tide mark is inundated by the sea except during low tide. This means that the heads in this well almost equal the tidal variation of the sea level. The mean fresh water head in this well is thus the mean sea level of 2.36 mTAW corrected for the density of sea water. The observation well placed just below the high tide mark is only inundated by the sea during high tide. During ebb, the fresh water head decreases slowly because of the descending water table. This decrease of the water table is very slow due to the small average interstitial velocity of the groundwater and the large specific yield. Mean fresh water head in this well is therefore 3.93 mTAW which is much higher than the mean sea level but lower than the high tide level. During the inundation of the observation well placed on the mean sea level mark the tidal fluctuation of the sea level is measured. On some point during the ebb

 DOI 10.1007/s10040-005-0446-5

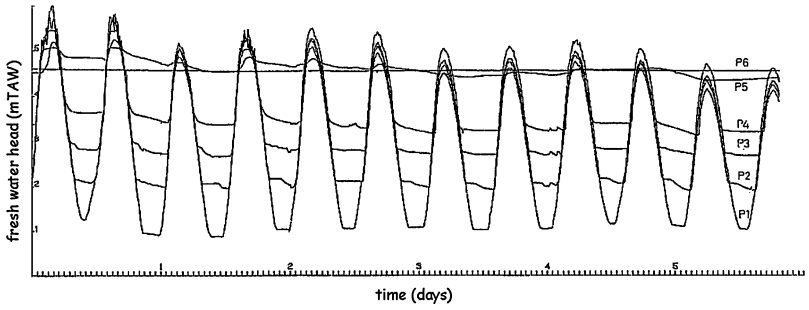

Fig. 4 Fluctuation of fresh water heads measured in observation wells P1 to P6. The graph starts at 11 h15 local time (0 h) on 22/03/81. Measurements show the response to the tides when the well's location is inundated causing a peak, a rapid decline, and then a very slow decrease in head until the next rise

this place is no longer inundated by the sea and the fresh water heads decrease slowly. This is again the slow decrease of the water table which is measured until this location is inundated by the sea. Although the elevation head of the location equals the mean sea water level, the mean time averaged fresh water head is larger (2.99 mTAW). On the shore, there is thus a step descent of the fresh water heads from the back shore towards the fore shore which is a constant gradient over a long time period. The values for these constant fresh water heads were deduced from measurements on the shore (Lebbe 1981). Fresh water heads were measured in observation wells indicated on Fig. 2 during 6 days (Fig. 4) and used to calculate the constant fresh water heads on the shore. The seaward vertical boundary is also a constant head boundary. The salt water heads are the same over the whole depth (2.36 mTAW) and the corresponding fresh water heads were calculated. Water which enters the model through the constant heads on the shore and in the sea is salt water with at TDS of 27000 mg/l.

Because the aquifer is rather homogeneous close to the French-Belgian border, all layers of the numerical model are given the same parameter values. These values are based on the calibration of a previous model using the observed heads and the fresh-salt water distribution (Lebbe 1999). Horizontal hydraulic conductivity is 10.0 m/d and vertical hydraulic conductivity is 0.1 m/d. Longitudinal, horizontal transverse and vertical transverse dispersivity are 0.2 m, 0.02 m and 0.002 m respectively. Effective porosity is 0.38. At the beginning of the simulation, the groundwater reservoir is completely filled with salt water. This salt water has a TDS (total dissolved solids) of 27000 mg/l and a density of 1019 kg/m^3. The fresh water infiltrating in the dune area has a TDS of 500 mg/l and a density of 1000 kg/m^3, resulting in a buoyancy of 0.019. For the first simulation a time period of 500 years is simulated. It corresponds with one stress period divided in 4000 time steps of 0.125 year each. After each time step, the groundwater flow is recalculated taking into account the salt-fresh water distribution from the previous time step. Sixteen particles are placed per cell and the maximum fresh water head change criterion for convergence is 0.1 mm.

Simulation results and discussion

Figure 5 shows the results of the simulations. After 20 years the beginning of the formation of a fresh water lens is visible under the dunes. Salt water is replaced by fresh infiltration water and the beginning of the formation of the fresh water tongue under the shore is already present. An important flow of fresh water exists from the dunes under the shore towards the sea. This flow drives the development of the fresh water tongue. Above it, salt water infiltrates on the back shore and flows out on the fore shore and under the sea. This cycle will lead to the development of a salt water lens above the fresh water tongue. After 80 years, salt water in the dune area is almost completely replaced by fresh infiltration water. Fresh water discharges on the seabed and a salt water lens exists above the fresh water tongue. From about 200 years in the simulation, no important changes occur. This implies that the present-day observed inverse density distribution is in a dynamical equilibrium. The amount of infiltration and seepage, its water quality and some flow lines are given in Fig. 6 for the present-day situation. A relatively large amount of salt water (about 18 m^3/d) infiltrates on the back shore during high tides. This water forms the salt water lens and discharges on the fore shore and proximal part of the seabed. Discharge velocities of salt water range between 1.5 and 8.0 mm/d. The discharge velocities equal the average interstitial velocities of the upper model layer. These discharge velocities enlarge towards the sea. Fresh water infiltrating in the dune area flows under the salt water lens and discharges on the sea floor. A total of 4.14 m^3/d of fresh water infiltrates in the dune area. The same amount of fresh water discharges on the seabed with an average interstitial velocity of 3.2 mm/d. This is a relatively large velocity but still larger velocities can be observed (5 to 70 mm/d) as was found by Groen (2002) in literature.

The cycle of infiltration during high tide on the back shore and discharge during low tide on the fore shore is also described by Urish and McKenna (2004) for an embayment on Cape Cod, Massachusetts. In this case, salt water infiltrates during high tide pushing back the fresh groundwater. During ebb and during low tide fresh water coming from the land moves more seaward and can then discharge on the fore shore and on the seabed. The large movement of the fresh water is due to the large permeability (up to 125 m/d) of the groundwater reservoir. The tides are acting hereby as a pump pushing back the fresh water with the infiltration of salt water. No important salt water lens is, however, formed above the fresh water flowing from land towards the bay. The much smaller hydraulic conductivities at De Panne make the movement of the groundwater very slow, inhibiting a relevant movement of the fresh water land-

 DOI 10.1007/s10040-005-0446-5

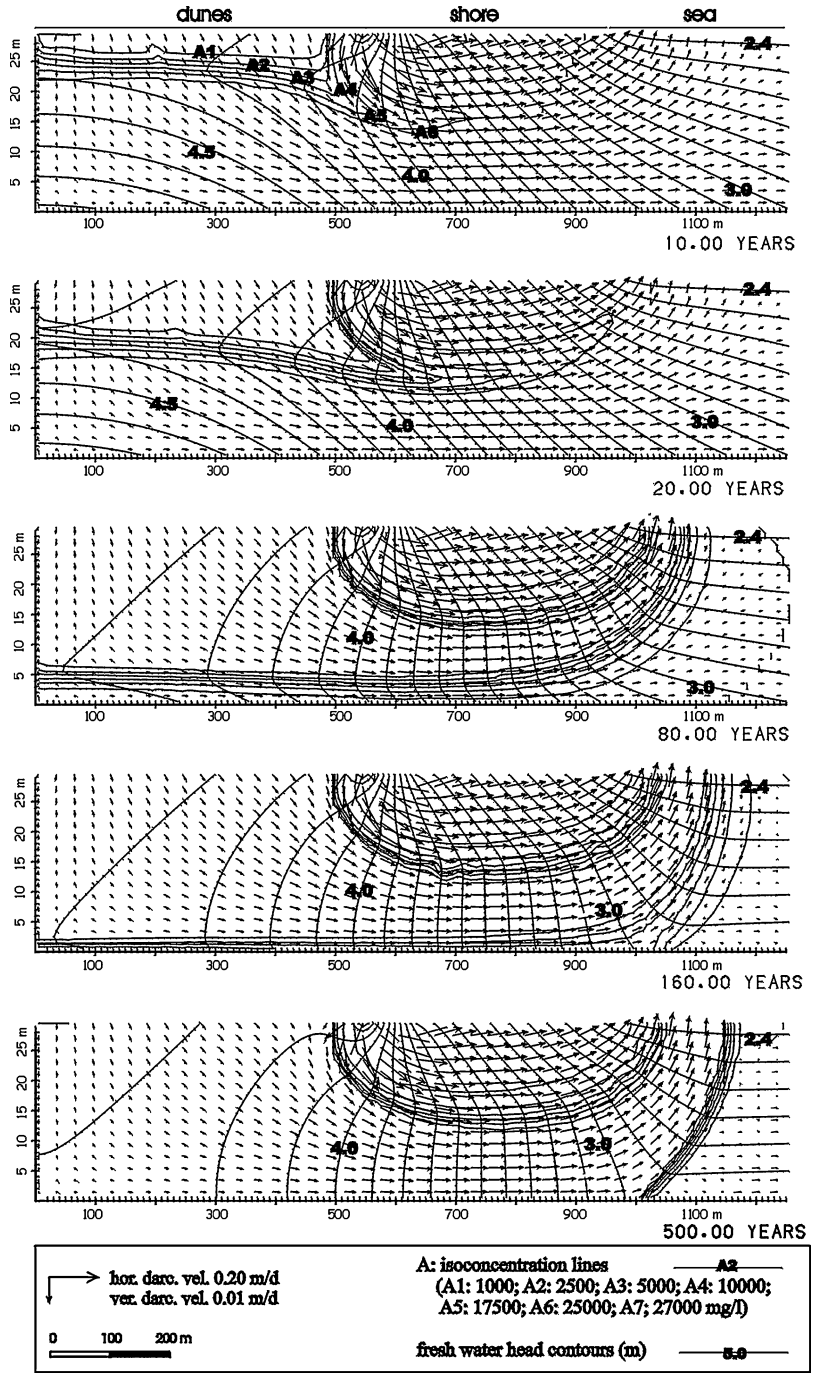

Fig. 5 Simulated evolution of the groundwater flow and water quality distribution under the dunes, shore and sea along the French-Belgian border

or seawards during the course of one tidal cycle. A larger amount of salt water infiltrates at De Panne on the back shore which means that a large salt water lens can develop under the shore. This clearly illustrates that the water quality distribution at the shore of De Panne is due to the long term boundary conditions (time averaged hydraulic heads influenced by the tides and the water table) on the shore and sea and not directly to the daily tides.

Figure 6 also gives an indication about the travel times of water particles. Water that infiltrates close to the dune's water divide has the largest residence time in the ground water reservoir, over 130 years. Water infiltrating more seaward has a smaller residence time than water infiltrating more landward. Residence time of water infiltrating on the dune-shore boundary has for instance a residence time of only 15 years. Salt water infiltrating on the back shore has the shortest residence times, between 1 and 15 years. Overall residence times are small. This along with the geological history explains very well the base exchange indexes being zero for all water samples. The young dunes started to form during the 7th and 8th century. From then on, mainly fresh water infiltrated the groundwater reservoir in the dunes. Salt water infiltrated only occasionally during severe storms when tidal inlets breached the dune

 DOI 10.1007/s10040-005-0446-5

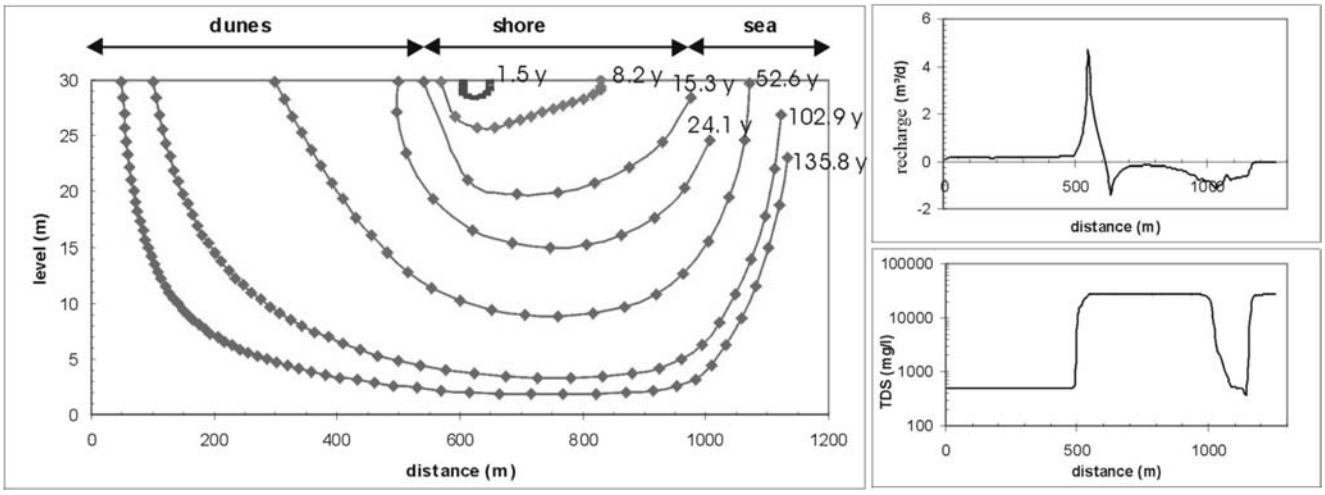

Fig. 6 Pathways followed by the infiltration water (main figure). Positions are given every 800 days except for the infiltration under the shore. Positions are given every 200 days for the 8.2 year line and every 50 days for the 1.5 year line. Figures at right give the recharge velocity (positive is infiltration, negative is seepage) and total dissolved solids (TDS) of the water in the first layer of the model

belt. Additionally, the low laying adjacent polder area was completely proclaimed from the 12th century on. The current groundwater flow system has thus been in existence more or less unaltered for at least 800 years. This means that the sediments were flushed several times by fresh or salt water, respectively in the fresh water tongue and salt water lens. Chemical equilibrium between the pore water and sediments was therefore reached and no base exchange is occurring.

Altering the shore's boundary conditions

Geomorphology of the shore and tidal range stipulate the observed water quality distribution. These conditions determine the amount of salt water which infiltrates on the back shore and thus the extent of the salt water lens. This also influences the shape of the fresh water tongue. Furthermore, the aquifer must be permeable. If a thick shallow semi-permeable layer was present under the shore, no salt water would infiltrate restricting the formation of the salt water lens. In this section, the influence of shore width and tidal range are simulated and compared to the reference situation depicted in Fig. 5.

In a first simulation, the tidal range is halved. The mean sea level of 2.36 mTAW remains. The resulting groundwater flow and water quality distribution are given in Fig. 7a. The fresh water heads on the shore are now smaller ranging from 2.36 mTAW on the low water line to 3.54 mTAW on the dune/shore transition. The width of the shore does not change (420 m). Therefore the gradient is smaller and less water infiltrates on the back shore, only about 6.3 m^3/d. This is almost three times less than in the reference situation. The result is that the salt water lens becomes smaller, both in width and in depth and the discharge velocities also decrease (between 1.5 and 4.3 mm/d). Therefore, the extent of the fresh water tongue enlarges. The tongue's discharge zone becomes wider and is situated on the fore shore and below the low water line. The discharge rate is about 2.1 mm/d. Average interstitial velocity of the fresh water tongue is smaller than in the reference situation because of the larger discharge zone. Notice that the transition zone between the fresh water tongue and salt sea water is less steep than in the reference situation. The outflow of fresh water is also more tangential to the seabed.

In a second simulation, the width of the shore is halved. In comparison with the reference situation a large hydraulic gradient (from 4.5 mTAW on the dune/shore transition to 2.36 mTAW on the low water line) is present due to the shorter shore (210 instead of 420 m). A large amount of salt water (about 24.0 m^3/d) infiltrates on the back shore. Therefore, a relatively large salt water lens is present (Fig. 7b). Water infiltrating on the back shore discharges on the fore shore and in a large zone on the sea bed. Discharge rate of the fresh water is about 2.9 mm/d. Discharge rates of salt water are relatively large, between 1 and 31 mm/d. The transition zone between the fresh water tongue and salt water lens is relatively large. The transition zone is also pushed back in the dune area. Salt water infiltrating on the upper part of the back shore and flowing initially landward is mixed with fresh water infiltrating in the dune area. This results in the larger transition zone.

Finally, two situations having the same model set-up are simulated. A constant hydraulic head of 2.36 mTAW is present in the first layer from 550 m to 1260 m. This is the case in a situation where no tides are present. The sea is at a constant level of 2.36 mTAW. The rest of the model (from 0 to 550 m) represents the dunes and perhaps a small shore which is never inundated by the tides and where fresh water thus can infiltrate. The same schematisation can be used for a situation where no shore is present. Sea water level changes, due to tides, and fluctuates against a natural (cliff) or manmade (dike) barrier. Even during low tide, the area seaward from the barrier remains inundated. The mean sea level is 2.36 mTAW. In these cases, a typical

 DOI 10.1007/s10040-005-0446-5

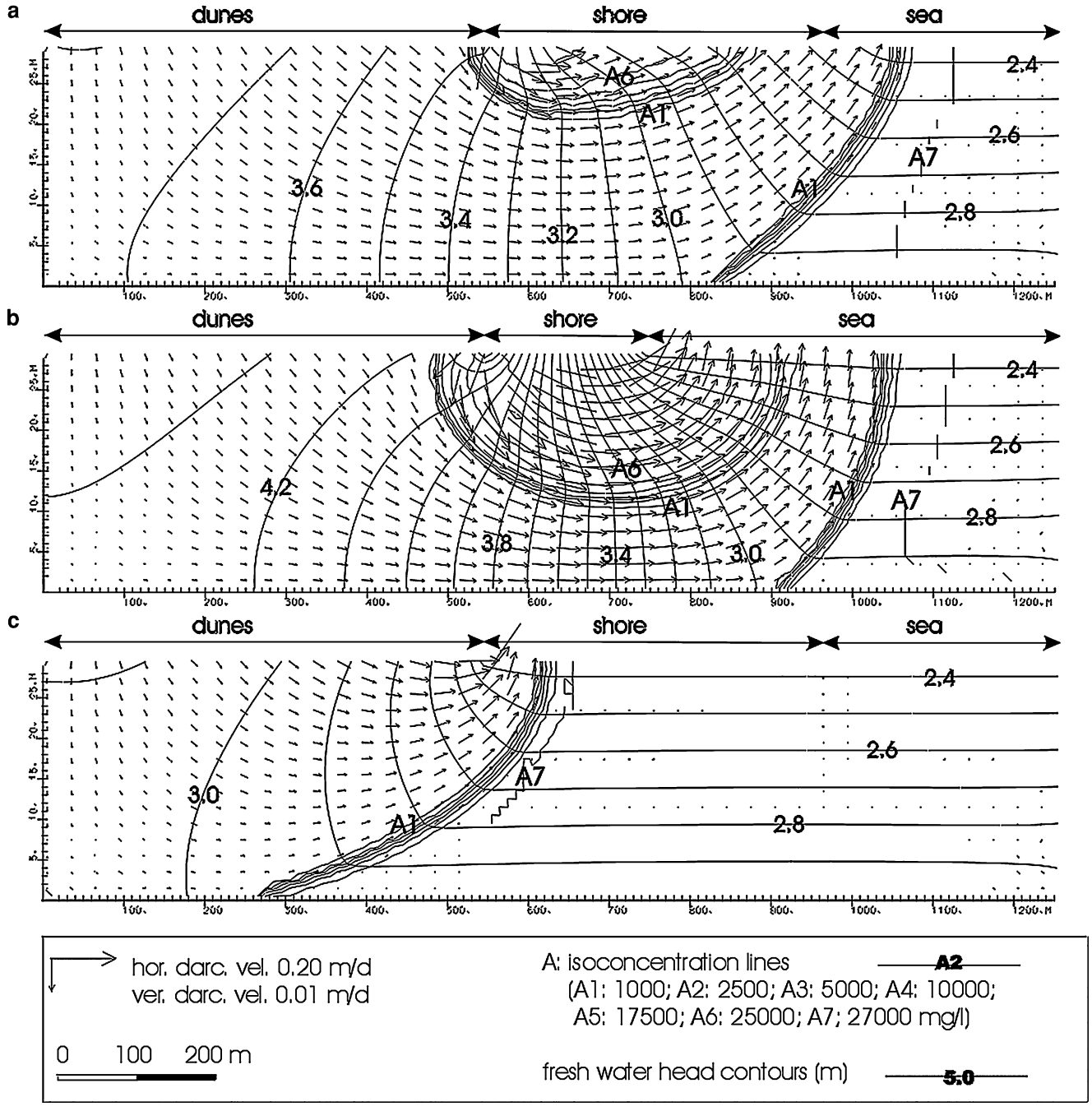

Fig. 7 Groundwater flow and water quality distribution in the case of the tidal range being halved (**a**), the width of the shore being halved (**b**) or no tides and/or no shore is present (**c**)

textbook picture of water quality distribution is obtained (Fig. 7c). Fresh water infiltrates on land and flows towards the sea. Where sea water meets this fresh water a typical salt water wedge under the fresh water lens develops. Fresh water discharges on the adjacent seabed with a rate of about 4.1 mm/d.

Influence of a semi-pervious layer

In this section a semi-permeable layer of 1 m thickness (1 model layer) is included in the simulations. Its horizontal hydraulic conductivity is 0.4 m/d and its vertical conductivity is 0.004 m/d. This is 25 times smaller than the surrounding sediments. The model is enlarged seaward by 300 m. Three different positions for this layer are considered. In a first simulation the semi-pervious layer is situated in layer 1. Simulation results are given in Fig. 8a. Three important differences with the reference situation are notable. First, the salt water lens is much shallower due to a smaller infiltration of salt water on the shore (6.5 m^3/d). The width of its discharge region remains more or less the same, so the discharge rates are also smaller (between 0.1 and 5.0 mm/d)

 DOI 10.1007/s10040-005-0446-5

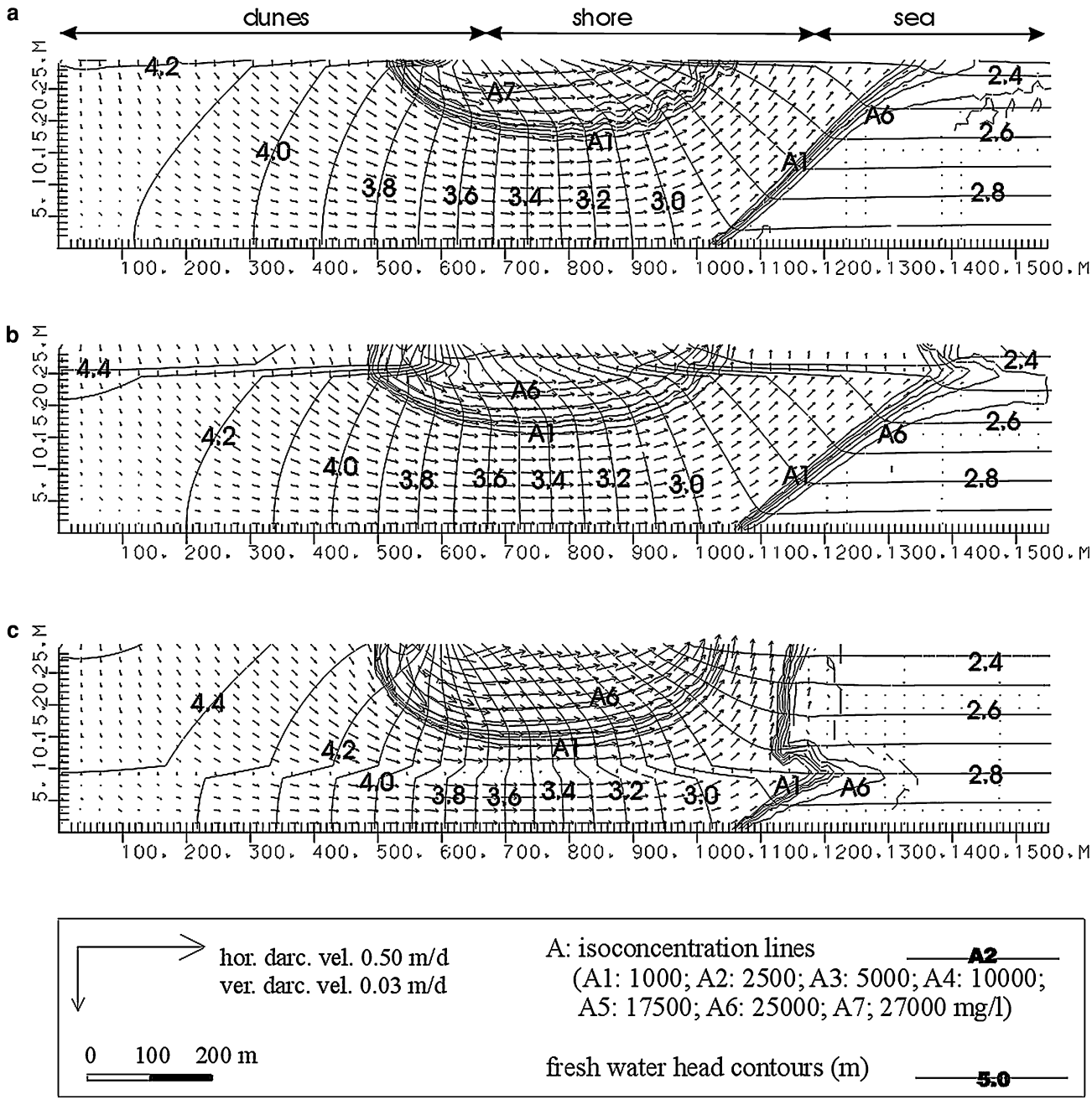

Fig. 8 Groundwater flow and water quality distribution in the case of a semi-permeable layer in model layer 1 (**a**), model layer 5 (**b**) and model layer 20 (**c**)

than in the reference situation. Secondly, the extent of the fresh water tongue enlarges. It becomes thicker because less salt water infiltrates on the shore. The discharge zone enlarges seaward due to the semi-permeable layer. The same amount of fresh water infiltrates in the dunes as in the reference situation but the semi-permeable layer hinders the discharge of this fresh water and the discharge zone becomes therefore wider. Discharge rates of fresh water are also diminished to 1.2 mm/d. Finally the transition zones between fresh and salt water are altered especially between the fresh water tongue and the salt sea water. This transition zone is straightened and becomes less steep. Additionally it widens towards the semi-permeable layer. Streamlines are more tangential to the seabed than in the reference situation. If the semi-permeable layer is thicker or/and its conductivity is smaller, no salt water would be able to infiltrate in the groundwater reservoir. Therefore no salt water lens would be formed. This is the kind of situation which is described by Krantz et al. (2004) and Manheim et al. (2004) in the coastal bays of the Delmarva Peninsula, Maryland and Virginia. Here fresh water flowing from land towards the bays is overlain by a thick layer of salt water in a semi-permeable layer.

 DOI 10.1007/s10040-005-0446-5

In a second simulation, the semi-permeable layer is situated in model layer 5 (Fig. 8b). In comparison with the previous situation, double the amount of salt water infiltrates on the shore (13.3 m^3/d). Therefore, the salt water lens is larger. The influence of the semi-permeable layer on the transition zone between the fresh water tongue and the salt seawater is now apparent in the distortion of the iso-concentration lines. There is an important lateral flow component just beneath the semi-pervious layer. This leads to an extension of brackish water in but mostly underneath the semi-permeable layer. Finally, the semi-permeable layer is placed in layer 20 (Fig. 8c). This water quality distribution corresponds more with the reference situation. The same amount of salt water infiltrates on the shore and discharge velocities of fresh water are more or less the same. The major difference with the reference situation is found in the distal part of the fresh water tongue in the semi-pervious layer and its surroundings.

Concluding remarks

At the French-Belgian border an inversion density distribution occurs. A salt water lens exists under the shore underlain by fresh water. This water quality distribution shows that other distributions than the well-known salt water wedge under fresh water can exist in coastal areas. This situation is the result of three factors: shore morphology, tidal range and a permeable groundwater reservoir. In the Belgian situation, a relatively large tidal range is encountered. Additionally a wide shore with a gentle mean slope is present. Because of these, the horizontal range between the low and high water line is large. If a permeable groundwater reservoir is present, a small groundwater cycle comes into existence whereby salt water infiltrates on the back shore and discharges on the fore shore and/or on the seabed forming the salt water lens. This illustrates also that, in many cases, it is not the mean sea level which is of importance to understand the flow on the land-sea transition zone. The hydraulic gradient on the shore must be taken into consideration. Fresh water infiltrated on land, here in the dunes, is flowing under this salt water lens towards the sea. This inverse density distribution is in dynamical equilibrium. Although to the authors' knowledge, no similar water quality distributions (thick salt water lens above fresh water) are reported, many comparable hydrogeological situations are present in coastal areas all over the world. Similar water quality distributions are thus expected to be found. However, similar density distributions have been studied in the laboratory with sand tank experiments (Boufadel 2000; Robinson and Li 2004). These show also the development of a salt water lens above a fresh water tongue.

In case of a smaller tidal range, the hydraulic gradient on the shore is smaller and less salt water infiltrates on the back shore. Therefore, the salt water lens will be smaller. If only a small shore is present, tidal range dictates in a permeable groundwater reservoir the amount of salt water which infiltrates on the back shore and hence the dimensions of the salt water lens. In the case no shore or no tides are present, the water quality distribution is reduced to the classic distribution were a fresh water lens is found above a salt water wedge. Permeability of the groundwater reservoir is also of importance. A shallow semi-permeable layer restricts the amount of salt water which can infiltrate on the back shore and thus the dimensions of the salt water lens. A thick semi-permeable layer or one with a very low hydraulic conductivity inhibits the infiltration of salt water on the back shore. No salt water lens will be formed in this case. A shallow semi-permeable layer also hampers the upward flow of fresh water. The fresh water discharge zone under the fore shore or seabed becomes therefore wider. A brackish extension seaward also develops under the semi-permeable layer. Finally, the transition zone between the fresh water tongue and salt sea water is straighter and more inclined. If this semi-permeable layer is found deeper in the groundwater reservoir, the influence on water quality distribution is minimal. Its major impact is an extension seaward of brackish water in this layer and its surroundings. The classic distribution and the distribution along the French-Belgian border can thus be regarded as end members of a series of intermediate cases in function of shore morphology, tidal range and heterogeneity of the groundwater reservoir.

Acknowledgments The authors wish to thank dr. Maria Clara Castro, dr. Leonard Konikow and dr. Patrick Goblet for their constructive review of the paper.

References

Bear J (1972) Dynamics of fluids in porous media. Elsevier, Amsterdam

Boufadel MC (2000) A mechanistic study of nonlinear solute transport in a groundwater-surface system under steady state and transient hydraulic conditions. Water Resour Res 36(9):2546–2565

Cooper HH, Kohout FA, Henry HR, Glover RE (1964) Sea water in coastal aquifers. US Geol Survey Water Supply Papers 1613–C:1–84

Domenico PA, Schwartz FW (1998) Physical and chemical hydrogeology, 2nd edn. Wiley, New York

Freeze RA, Cherry JA (1979) Groundwater. Prentice-Hall, Englewood Cliffs, NJ

Groen K (2002) The effects of transgressions and regressions on coastal and offshore groundwater: a case study of Suriname and generic studies into groundwater flow systems, salinity patterns and paleogroundwater. PhD Dissertation, Vrije Universiteit, Amsterdam

Konikow LF, Bredehoeft JD (1978) Computer model of two-dimensional solute transport and dispersion in ground water. USGS Tech. of Water-Resources investigations, Book 7, Chapter C2

Konikow LF, Goode DJ, Hornberger GZ (1996) A three-dimensional method-of-characteristics solute-transport model (MOC3D). U.S.G.S. Wat Resour Invest Rep 96–4267

Krantz DE, Manheim FT, Bratton JF, Phelan DJ (2004) Hydrologic setting and ground water flow beneath a section of Indian River Bay, Delaware. Ground Water-Oceans Issue 42(7):1035–1051

Lebbe L (1978) Hydrogeologie van het duingebied ten westen van De Panne. PhD Thesis, Geological Institute, Ghent University. (Hydrogeology of the dune area west of De Panne; in Dutch)

 DOI 10.1007/s10040-005-0446-5

Lebbe L (1981) The subterranean flow of fresh and salt water underneath the western Belgian beach. 7th Salt Water Intrusion Meeting, Uppsala. Sver Geol Unders Rap Meddel 27:193–219
Lebbe L (1983) Mathematical model of the evolution of the fresh water lens under the dunes and beach with semi-diurnal tides. 8th Salt Water Intrusion Meeting, Bari. Geologia Applicata e Idrogeologia, volume XVIII, parte II, 211–226
Lebbe L (1999) Parameter identification in fresh-saltwater flow based on borehole resistivities and freshwater head data. Adv Water Resour 22(8):791–806
Manheim FT, Krantz DE, Bratton JF (2004) Studying ground water under Delmarva coastal bays using electrical resistivity. Ground Water-Oceans Issue 42(7):1052–1068
Oude Essink GHP (2001) Salt Water Intrusion in a Three-Dimensional Groundwater System in The Netherlands: A Numerical Study. Transp Porous Media 43(1):137–158
Pranzini G (2002) Groundwater salinization in Versilia (Italy). Proc. 17th Salt Water Intrusion Meeting, Delft, The Netherlands, 6–10 may 2002):412–421
Robinson C, Li L, (2004) Effect of tidal oscillations on water exchange and mixing in a coastal aquifer. Proc. of 15th International Conference on Computational Methods in Water Resources, Chapel Hill, North Carolina, USA, 1583–1594
Rushton KR (2003) Groundwater hydrology: conceptual and computational models. Wiley, New York, 416pp
Stuyfzand PJ (1986) A new hydrochemical classification of water-types: principles and application to the coastal dunes aquifer system of the Netherlands. Proceedings SWIM 9, Delft. 641–655
Stuyfzand PJ (1993) Hydrochemistry and Hydrology of the Coastal Dune area of the Western Netherlands. PhD Thesis, Nieuwegein, KIWA, Afd. Onderzoek & Advies
Urish D, McKenna TE (2004) Tidal effects on ground water discharge through a sandy marine beach. Ground Water-Oceans Issue 42(7):971–982
Vandenbohede A (2003) Solute transport in heterogeneous aquifers: parameter identification and its use in groundwater pollution and salt water intrusion problems. Ph.D. thesis, Ghent University

 DOI 10.1007/s10040-005-0446-5